Am J Physiol Regul Integr Comp Physiol 294: R993–R1003, 2008.
First published January 2, 2008; doi:10.1152/ajpregu.00695.2007.

Differential localization and regulation of two aquaporin-1 homologs in the intestinal epithelia of the marine teleost *Sparus aurata*

Demetrio Raldúa, David Otero, Mercedes Fabra, and Joan Cerdà

Laboratory Institut de Recerca i Tecnologia Agroalimentàries-Institute of Marine Sciences, Cousejo Superior de Investigaciones Cientificas, Barcelona, Spain

Submitted 26 September 2007; accepted in final form 27 December 2007

Raldúa D, Otero D, Fabra M, Cerdà J. Differential localization and regulation of two aquaporin-1 homologs in the intestinal epithelia of the marine teleost *Sparus aurata. Am J Physiol Regul Integr Comp Physiol* 294: R993–R1003, 2008. First published January 2, 2008; doi:10.1152/ajpregu.00695.2007.—Aquaporin (AQP)-mediated intestinal water absorption may play a major osmoregulatory role in euryhaline teleosts, although the molecular identity and anatomical distribution of AQPs in the fish gastrointestinal tract is poorly known. Here, we have investigated the functional properties and cellular localization in the intestine of two gilthead seabream (*Sparus aurata*) homologs of mammalian aquaporin-1 (AQP1), named SaAqp1a and SaAqp1b. Heterologous expression in *Xenopus laevis* oocytes showed that SaAqp1a and SaAqp1b were water-selective channels. Real-time quantitative RT-PCR and Western blot using specific antisera indicated that abundance of SaAqp1a mRNA and protein was higher in duodenum and hindgut than in the rectum, whereas abundance of SaAqp1b was higher in rectum. In duodenum and hindgut, SaAqp1a localized at the apical brush border and lateral membrane of columnar enterocytes, whereas SaAqp1b was detected occasionally and at very low levels at the apical membrane. In the rectum, however, SaAqp1a was mainly accumulated in the cytoplasm of a subpopulation of enterocytes spread in groups over the surface of the epithelia, including the intervillus pockets, whereas SaAqp1b was detected exclusively at the apical brush border of all rectal enterocytes. Freshwater acclimation reduced the synthesis of SaAqp1a protein in all intestinal segments, but it only reduced SaAqp1b abundance in the rectum. These results show for the first time in teleosts a differential distribution and regulation of two functional AQP1 homologs in the intestinal epithelium, which suggest that they may play specialized functions during water movement across the intestine.

gilthead seabream; SaAqp1a; SaAqp1b; functional expression; salinity; gastrointestinal tract

OSMOREGULATION IN TELEOST fish is achieved by integrating ion and water transport mechanisms in the gills, kidney, gastrointestinal tract, and urinary bladder (5, 9). To compensate for osmotic water loss and dehydration, marine teleosts drink relatively large amounts of seawater (SW), absorb most of this water and monovalent ions across the intestine, secrete excess of ions from gill chloride cells, and excrete a modest amount of near-isoosmotic urine (17). Ingested SW is mainly desalted in the esophagus, which absorbs Na^+ and Cl^- through both passive and active transport pathways, and thereafter along the entire length of the intestine by active transport of monovalent ions in the blood (17, 18, 36). The subsequent water absorption takes place in the intestine by osmotic mechanisms following active absorption of monovalent ions (17, 44, 45). Thus, in euryhaline fish, intestinal water absorption is critical for water balance, especially when fish acclimate to SW during their life cycle (4, 9, 17). However, it is yet unclear whether water in the fish intestine is absorbed through transcellular or paracellular routes and which water-specific carrier proteins may play a direct role in water movement.

The molecular water channels or aquaporins (AQPs) are members of the major intrinsic proteins (MIP) family of integral membrane proteins that exists in virtually every living organism (1). These proteins are structurally related and function as water channels involved in fluid transport within various organs, although some of them are also permeable to small solutes, such as glycerol and urea (aquaglyceroporins). The AQPs consist of six transmembrane (TM) domains connected by five loops (A–E) and have their NH_2 and COOH terminus located intracellularly. One molecule consist of two repeats, which are 180° mirror images of each other, and each repeat contains the highly conserved asparagine-proline-alanine (NPA) motif (in loops B and E), which is the hallmark of the MIP family of proteins to which AQPs belong. The folding of loops B and E is important for the formation of the water pore, since it has been corroborated by the determination of the three-dimensional structure of AQP0, AQP1, and AQP9 (16).

The potential role of AQPs in water transport across the gastrointestinal tract of teleosts has been recently investigated. Although few cDNAs encoding fish AQPs have been isolated so far, a number of studies have demonstrated the presence of mRNA and/or protein of aquaporin-1 (Aqp1), aquaporin-3 (Aqp3), and of two aquaglyceroporins, named AQPe and sbAQP, in the esophagus, stomach, and/or intestine of several teleosts (4, 10–12, 15, 20, 29, 36–38, 43, 50). In catadromous teleosts, such as the European eel (*Anguilla anguilla*) and Japanese eel (*A. japonica*), Aqp1 is found at the apical membrane of intestinal columnar enterocytes, and transition from freshwater (FW) into SW, as well as treatment of fish with the "SW-adapting" hormone cortisol, upregulates Aqp1 synthesis in epithelial cells of all intestinal segments (4, 36). In agreement with this, FW acclimation of the marine teleost sea bass (*Dicentrarchus labrax*) downregulates *aqp1* mRNA expression in intestinal epithelial cells (15). These observations thus suggest that fish Aqp1 may play a pivotal role in the control of intestinal water absorption in teleosts under SW conditions.

The gilthead seabream (*Sparus aurata*) is a marine teleost that inhabits coastal waters, capable of adapting to considerable changes in environmental salinity (31). Previous studies with this species showed that a decrease in salinity activates the

Address for reprint requests and other correspondence: J. Cerdà, Lab IRTA-ICM, CMIMA-CSIC, Passeig Marítim 37-49, 08003-Barcelona, Spain (e-mail: joan.cerda@irta.es).

The costs of publication of this article were defrayed in part by the payment of page charges. The article must therefore be hereby marked "*advertisement*" in accordance with 18 U.S.C. Section 1734 solely to indicate this fact.

release of the "FW-adapting" hormone prolactin, growth hormone, and melatonin (25, 32, 34); induces changes in gill Na^+-K^+-ATPase and thyroid hormone-metabolizing enzymes and thyroid plasma levels (24, 28); and leads to transitory blood hypomineralization (30). Additionally, prolactin and cortisol control the Na^+-K^+-ATPase activity and blood osmolality in fish maintained in brackish water, thus improving its hypoosmoregulatory capacity (27, 33, 35). However, in this species, as well as in other marine teleosts, there is no information on the cellular localization of AQPs in the gastrointestinal tract and the effects of changes in salinity.

In the seabream, we have recently isolated the cDNAs encoding two AQP homologs of mammalian AQP1, called *S. aurata* Aqp1 (SaAqp1) and *S. aurata* Aqp1 of the ovary (SaAqp1o). The corresponding genes have been found in other teleosts (7, 47), and they seem to be evolved from a teleost-specific local duplication of an ancestral *AQP1* gene during evolution; accordingly, they should be named Aqp1a and Aqp1b, respectively (7, 13, 47). In the seabream, both orthologs show a completely distinct pattern of expression, although SaAqp1a is present in most organs, including the intestine, gills, and kidney and SaAqp1b is found predominantly in the oocyte, where it is involved in water uptake during meiotic maturation (13, 14, 47). In the present work, we show that SaAqp1a and SaAqp1b are both functional water channels when expressed in *Xenopus laevis* oocytes and that SaAqp1b is in fact synthesized by intestinal epithelial cells, as is SaAqp1a, in addition to the oocyte. However, the cellular localization of both AQPs along the entire length of the intestine, as well as the changes in protein abundance under different salinity conditions (SW and FW), appeared to be different.

MATERIALS AND METHODS

Fish. Gilthead sea bream juveniles (100–300 g in body wt), reared in captivity at the Center of Aquaculture IRTA and acclimated in SW, were divided into two groups ($n = 20$) and placed in 1,500-liter tanks. One tank was maintained in SW (30‰ salinity) while the other was in FW (1–2‰ salinity). Both SW- and FW-acclimated fish were starved and maintained under natural conditions of photoperiod (1212-h light-dark cycle) and temperature (20°C) for 10 days before a subsample of fish ($n = 6$) was killed. Fish were sedated with 100 ppm phenoxyethanol and immediately killed by decapitation. Pieces (~100 mg) of the duodenum, hindgut, and rectum were frozen in liquid nitrogen and stored at −80°C or fixed for immunohistochemistry. All procedures for the killing of fish were approved by the Ethics and Animal Experimentation Committee from IRTA (Spain).

Antibodies. Commercially prepared (Cambridge Research Biochemicals) specific antisera against SaAqp1a were raised in rabbits by immunization with a synthetic peptide corresponding to the COOH termini of the corresponding deduced amino acid sequence GDYDVNGGNDATAVEMTSK (GenBank accession no. AY626939). The antisera was affinity purified on thiopropyl Sepharose 6B coupled to the synthetic peptide. The specificity of the resulting fraction was tested by enzyme-linked immunosorbent assay and by immunofluorescence microscopy and Western blot of *X. laevis* oocytes expressing SaAqp1a. Production of antisera against a synthetic peptide corresponding to the COOH termini of SaAqp1b, PREGNSSPGPSQGPSQWPKH (GenBank accession number AY626938), has been described previously (13).

Functional expression in X. laevis oocytes. Transcription of pT7Ts-SaAqp1a and pT7Ts-SaAqp1b constructs and isolation, defolliculation, and injection of *X. laevis* oocytes were done as described previously (13). The osmotic water permeability (P_f) was measured from the time course of osmotic oocyte swelling in a standard assay. Oocytes were transferred from 200 mosmol/l modified Barth's medium (MBS) to 20 mosmol/l MBS medium at room temperature, and the swelling of the oocytes was followed under a stereomicroscope using serial images at 2-s intervals during the first 20-s period. The P_f values were calculated as described (43). To examine the effect of mercury on the P_f, oocytes injected with 1 ng SaAqp1a cRNA or 2 ng SaAqp1b cRNA were incubated in MBS containing 0.7 mM $HgCl_2$ for 15 min before the swelling assay, which was also performed in the presence of $HgCl_2$. To determine if the mercurial effect was reversible, the same oocytes were rinsed three times in MBS, incubated with 5 mM β-mercaptoethanol for 15 min, and subjected to the swelling assays 2 h later. The apparent glycerol permeability coefficient (P'_{gly}) of water-, SaAqp1a-, and SaAqp1b-injected oocytes was determined from oocyte swelling as described (43).

Real-time quantitative RT-PCR. The abundance of seabream *aqp1a* and *aqp1b* transcripts in the different regions of the intestine was determined by real-time quantitative RT-PCR (qPCR). Total RNA was extracted from samples of duodenum, hindgut, and rectum ($n = 3$ fish) with the RNeasy Mini kit (Qiagen). After DNase treatment with DNase I using the RNase-Free DNase kit (Qiagen), 1 μg of total RNA from each intestinal region (in triplicate) from each fish was reverse transcribed into cDNA using 10 IU Moloney murine leukemia virus-RT enzyme (Roche), 0.5 μM oligo$(dT)_{12–18}$ (Invitrogen), and 1 mM dNTPs, in a 20-μl volume reaction, for 1.5 h at 50°C. Real-time qPCR amplifications were performed in a final volume of 20 μl with 10 μl SYBR Green qPCR master mix (Applied Biosystems), 2 μl diluted (1:10) cDNA, and 0.5 μM of each forward and reverse primer. For *aqp1a*, the forward and reverse primers were 5′-GGCTCTCACGTACGATTTCC-3′ and 5′-TCTGTGTGGGACTATTTTGACG-3′, respectively, which amplified a fragment of 153 bp. For *aqp1b*, the forward oligonucleotide primer was 5′-GCGACGGAGTGATGTCAAAGG-3′, and the reverse primer was 5′-AGATAAGAGCCGCCGCTATGC-3′, which amplified a fragment of 203 bp. Both primer pairs were located flanking the last intron to exclude genomic contamination. The sequences were amplified in duplicate for each cDNA on 384-well plates using the ABI PRISM 7900HT sequence detection system (Applied Biosystems). The amplification protocol was as follows: and initial denaturation and activation step at 50°C for 2 min and 95°C for 10 min, followed by 40 cycles of 95°C for 15 s and 63°C for 1 min. After the amplification phase, a temperature-determining dissociation step was carried out at 95°C for 15 s, 60°C for 15 s, and 95°C for 15 s. For normalization of cDNA loading, all samples were run in parallel using 18S ribosomal protein (*18S*) as reference gene (GenBank accession number EF126042). Forward primer was 5′-GAATTGACGGAAGGGCACCACCAG-3′, and reverse primer was 5′-ACTAAGAACGGCCATGCACCACCAC-3′, which amplified a 148-bp fragment. To estimate efficiencies, a standard curve was generated for each primer pair from 10-fold serial dilutions (from 100 to 0.01 ng) of a pool of first-stranded cDNA template from all samples. Standard curves represented the cycle threshold value as a function of the logarithm of the number of copies generated, defined arbitrarily as one copy for the most diluted standard. All calibration curves exhibited correlation coefficients >0.99, and the corresponding real-time PCR efficiencies were >99%.

Western blotting. Total membranes were isolated from water-, SaAqp1a- and SaAqp1b-injected *X. laevis* oocytes (10 oocytes), as well as from pieces (~100 mg) of duodenum, hindgut, and rectum of seabream maintained in SW and FW. Tissues were homogenized in buffer containing 20 mM Tris, pH 7.4, 5 mM $MgCl_2$, 5 mM NaH_2PO_4, 1 mM EDTA, 80 mM sucrose, and cocktail of protease inhibitors (Mini EDTA-free; Roche) and centrifuged for two times 5 min each at 200 *g* at 4°C (23). Total membranes were isolated by a final 20-min centrifugation step at 13,000 *g* at 4°C and resuspended in 1% Nonidet P-40, 1 mM $CaCl_2$, 150 mM NaCl, 10 mM Tris, pH 7.4, and protease inhibitors. An aliquot of the homogenate was kept for

determination of protein concentration using the Bio-Rad Protein assay kit, and the rest was mixed with 2× Laemmli sample buffer (26) and frozen at −80°C. For immunoblotting, a volume of Laemmli-mixed homogenate corresponding to 0.2 oocyte equivalents or 20 μg of total protein was subjected to electrophoresis on 12% SDS-PAGE. Proteins were blotted on polyvinylidene difluoride membranes (Bio-Rad Laboratories) in high-glycine transfer buffer (190 mM glycine, 250 mM Tris, pH 8.6, and 20% methanol). Membranes were blocked for 1 h at room temperature in 5% nonfat dried milk in Tris-buffered saline with 0.1% Tween and incubated overnight (1:300) with SaAqp1a or SaAqp1b rabbit antisera. Bound antibodies were detected with goat anti-rabbit IgG antibodies (1:8,000) coupled to horseradish peroxidase using enhanced chemiluminescence (ECL detection system; Amersham). Control membranes were incubated with the antisera preadsorbed with a 30-fold molar excess of the corresponding immunizing peptides. For quantitation of SaAqp1a and SaAqp1b protein abundance, three separate membranes (for the duodenum, hindgut, and rectum), each containing samples of both SW- and FW-acclimated fish, were incubated with each antisera in duplicate. The signal intensity of SaAqp1a and SaAqp1b reactive bands was optimized for each intestinal segment by exposing each membrane to X-ray films for different times. The density of the bands was measured using the Quantity-One software (Bio-Rad Laboratories).

Immunofluorescence light microscopy. X. laevis oocytes injected with water and with SaAqp1a or SaAqp1b cRNAs and pieces of seabream duodenum, hindgut, and rectum were fixed in Bouin's without acetic acid (for SaAqp1a detection) or 4% paraformaldehyde in PBS (for SaAqp1b detection) for 4–6 h at room temperature and subsequently dehydrated and embedded in Paraplast (Sigma). Sections of ~6 μm were blocked with 5% goat serum in PBST (0.1% BSA and 0.01% Tween 20 in PBS) and incubated with SaAqp1a or SaAqp1b antisera (1:100) in PBST with 1% goat serum overnight at 4°C. Sections of duodenum and hindgut processed for SaAqp1b were permeabilized with 1% SDS in PBS for 10 min at room temperature before the blocking step. After four washes with PBS, 5 min each, the sections were incubated with fluorescein isothiocyanate anti-rabbit secondary antibodies (1:300 in PBS) for 1 h, washed three times with PBS, and mounted with Vectashield (Vector Labs). Control sections were incubated with the antisera previously incubated with the corresponding synthetic peptides as described above, or with the preim-

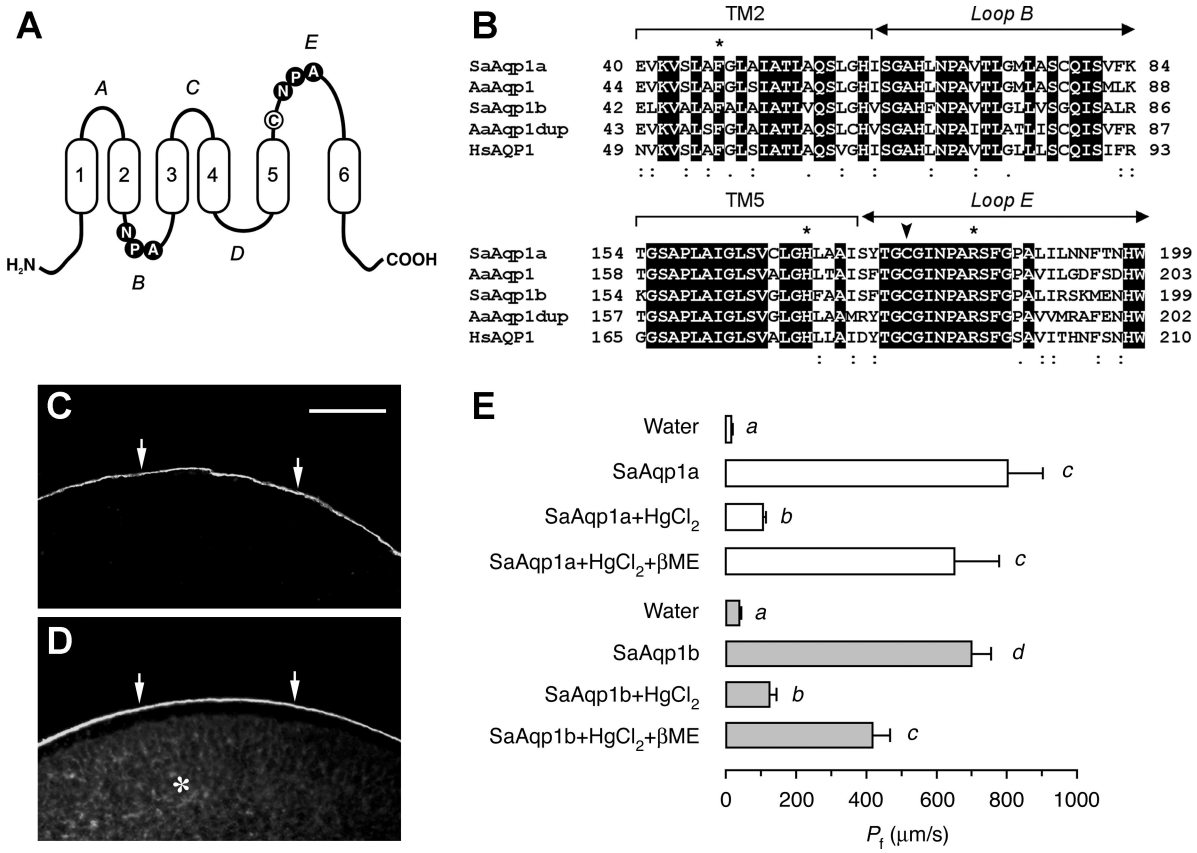

Fig. 1. Structural features and functional properties of *Spartus aurata* aquaporin (AQP) 1a and 1b (SaAqp1a and SaAqp1b, respectively). *A*: schematic diagram of AQP1 monomer showing the 6 transmembrane (TM) domains, the 2 asparagine-proline-alanine (NPA) motifs, and the Cys site involved in mercurial inhibition. *B*: amino acid sequence alignment of TM 2 and TM 5, and loops B and E involved in the formation of the pore, of human AQP1 (HsAQP1), *S. aurata* Aqp1a (SaAqp1a) and Aqp1b (SaAqp1b), and *Anguilla anguilla* Aqp1 (AaAqp1) and Aqp1dup (AaAqp1dup). Identical amino acids are indicated in black boxes, whereas conserved and semiconserved substitutions are indicated by a double or single dot, respectively. The asterisks indicate the residues Phe[56], His[180], and Arg[195] (HsAQP1 numbering) of the pore-forming region that are conserved among water-selective AQPs, and the arrowhead points the mercury-sensitive Cys site. *C–D*: immunofluorescence microscopy of *Xenopus laevis* oocytes injected with SaAqp1a (*C*) or SaAqp1b (*D*) cRNAs and incubated with anti-SaAq1a or anti-SaAqp1b antisera, respectively. The arrows point to the plasma membrane, and the asterisk indicates the oocyte cytoplasm. Sections from water-injected oocytes incubated with either SaAqp1a or SaAqp1b antisera did not show any positive signal (not shown). Bar, 50 μm. *E*: osmotic water permeability (P_f) of *X. laevis* oocytes expressing SaAqp1a or SaAqp1b. Oocytes were injected with 50 nl of water containing 1 ng SaAqp1a cRNA or 2 ng SaAqp1b cRNA, or with 50 nl of distilled water only (control oocytes), 48 h before the experiments. P_f was calculated from the time course of osmotic swelling of oocytes, previously incubated with or without 0.7 mM $HgCl_2$, in a hypoosmotic medium. Recovery of $HgCl_2$ inhibition was performed by treatment of oocytes with 5 mM β-mercaptoethanol (βME) for 15 min after mercury exposure. Values are means ± SE (n = 10–15 oocytes) from 2 representative experiments. In each panel, bars with different superscripts are statistically significant (ANOVA, $P < 0.05$).

mune sera (data not shown). In both cases, no positive staining was observed, with only nonspecific autofluorescence in red blood cells (data not shown). Immunofluorescence was observed and documented with a Leica TCS SP confocal microscope.

Data analysis. The data on *aqp1a* and *aqp1b* mRNA levels and P_f of oocytes injected with water or with SaAqp1a or SaAqp1b cRNAs, in the presence or absence of $HgCl_2$ and β-mercaptoethanol, were analyzed by one-way ANOVA. The data on SaAqp1a and SaAqp1b protein abundance in the duodenum, hindgut, and rectum were analyzed with the Student's *t*-test. The level of significance was set at $P \leq 0.05$.

RESULTS

SaAqp1a and SaAqp1b are functional, water-selective AQPs. The deduced amino acid sequences of SaAqp1a and SaAqp1b cDNAs are most similar to mammalian AQP1, with SaAqp1a being slightly more similar to AQP1 (57–59% identity) than SaAqp1b (45–54% identity) (13). However, seabream SaAqp1a and SaAqp1b are only 60% identical, similarly as it occurs between Aqp1 and Aqp1dup from European eel (69% identity; see Ref. 37), which are the eel Aqp1a and Aqp1b orthologs, respectively (7, 15, 47). The comparison of the primary structure of AQP1-like polypeptides between human, seabream, and European eel indicated that teleost AQP1-related sequences show the six potential TM domains, the two NPA motifs, and the residues of the pore-forming region (Phe^{56}, His^{180}, and Arg^{195}; human AQP1 numbering) in TM2, TM5, and loop E that are conserved in water-selective AQPs (46) (Fig. 1, *A* and *B*). All the amino acid sequences also showed the Cys residue before the second NPA motif (Cys^{178} for SaAqp1a and SaAqp1b), which is the potential responsible site for the inhibition of water permeability by mercurial compounds (42).

The relatively high conserved amino acid sequence of TM2 and TM5, as well as of loops B and E, of SaAqp1a and SaAqp1b with respect to the corresponding regions of human AQP1 (Fig. 1*B*) suggested that both fish paralogs might encode functional water channels. To confirm this, *X. laevis* oocytes injected with cRNAs encoding SaAqp1a or SaAqp1b were compared with oocytes injected with 50 nl of water. Immunofluorescence microscopy confirmed that SaAqp1a and SaAqp1b cRNAs were translated into their respective polypeptides, which were translocated into the oocyte plasma membrane, although SaAqp1b appeared to be partially retained in the cytoplasm (Fig. 1, *C* and *D*). Coefficients of P_f were determined from rates of oocyte swelling after transfer to hypoosmotic MBS solution (Fig. 1*E*). Water-injected oocytes exhibited low water permeability, whereas the P_f of oocytes injected with 1 ng SaAqp1a cRNA increased by ~50-fold, and those injected with 2 ng SaAqp1b cRNA increased by 18-fold. The presence of 0.7 mM $HgCl_2$ reduced the P_f of both SaAqp1a- and SaAqp1b-injected oocytes by ~87 and 82%, respectively. For SaAqp1a oocytes, the inhibition was completely recovered by incubation of oocytes with 5 mM β-mercaptoethanol, whereas, for SaAqp1b oocytes, the treatment with β-mercaptoethanol partially reversed the mercurial inhibition (42% recovery). The P'_{gly} of oocytes expressing SaAqp1a or SaAqp1b was not different from that of control oocytes, indicating that SaAqp1a or SaAqp1b were not permeable to glycerol (data not shown). These data thus indicated that both SaAqp1a and SaAqp1b were functional water channels whose permeability properties resembled those of mammalian AQP1 (41).

Differential mRNA expression and protein abundance of SaAqp1a and SaAqp1b along the intestine. To investigate the presence of SaAqp1a and SaAqp1b in the different portions of the seabream intestine, we first determined the abundance of *aqp1a* and *aqp1b* mRNAs by qPCR (Fig. 2*A*). The results of these experiments indicated that *aqp1a* transcripts were equally abundant in duodenum and hindgut but they accumulated significantly less ($P < 0.01$) in rectum. On the contrary, *aqp1b* mRNAs in duodenum and hindgut were similar but significantly lower ($P < 0.01$) than those in rectum, thus showing an opposite distribution than that of *aqp1a*.

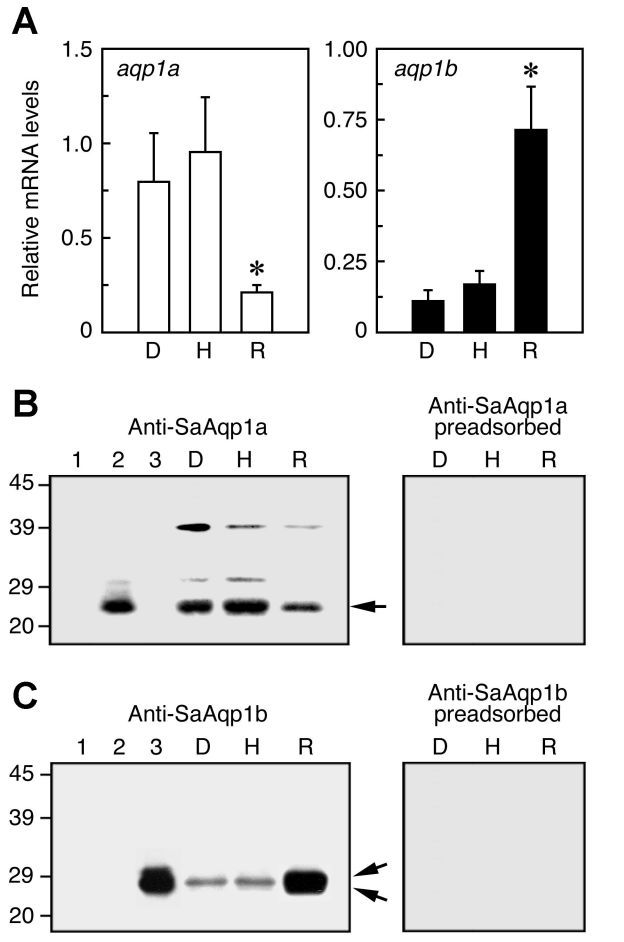

Fig. 2. Seabream *aqp1a* and *aqp1b* mRNA expression and protein abundance along the entire length of the intestine in seawater (SW)-acclimated fish. *A*: relative levels of *aqp1a* and *aqp1b* in the duodenum (D), hindgut (H), and rectum (R) determined by quantitative RT-PCR (qPCR). The levels were normalized to the *18S* gene and are presented as means ± SE ($n = 3$ fish). Bars with an asterisk are statistically different (ANOVA, $P < 0.01$). *B*: Western blot of membrane fractions from *X. laevis* oocytes (0.2 oocyte equivalents/lane) injected with water (*lane 1*), SaAqp1a (*lane 2*) or SaAqp1b (*lane 3*) and from duodenum (*lane D*), hindgut (*lane H*) and rectum (*lane R*) (20 μg/lane) using the SaAqp1a antisera. Blots were incubated with anti-SaAqp1a (*left*) or with anti-SaAqp1a preadsorbed with the synthetic peptide (*right*). The SaAqp1a reactive band of ~26 kDa, possibly corresponding to SaAqp1a monomer, is indicated by an arrow. *C*: Western blot of the same protein extracts in *B* probed with anti-SaAqp1b (*left*) or with anti-SaAqp1b preadsorbed with the immunizing peptide (*right*). The two very close SaAqp1b reactive bands, of ~27 and 29 kDa, are indicated by arrows. In *B* and *C*, apparent molecular masses (kDa) are indicated on the *left*.

Western blotting analysis on protein extracts from the different regions of the intestine was subsequently carried out using SaAqp1a- and SaAqp1b-specific antisera to detect the presence of the corresponding polypeptides (Fig. 2*B*). Immunoblotting on total membrane protein extracts from *X. laevis* oocytes injected with water or cRNAs encoding SaAqp1a or SaAqp1b, using the SaAqp1a antisera, showed a single protein band with a molecular mass of ~26 kDa in extracts from oocytes injected with SaAqp1a, thus being consistent with the molecular mass of SaAqp1a (26.1 kDa) calculated from the deduced amino acid sequence of its cDNA (Fig. 2*B*, *left*, *lane 2*). This band was absent in water- and SaAqp1b-injected oocytes (Fig. 2*B*, *left*, *lanes 1* and *3*). In the extracts from the three intestinal segments, the SaAqp1a-reactive band was also present, but its intensity was higher in the duodenum and hindgut than in the rectum (Fig. 2*B*, *left*, *lanes D, H*, and *R*). In protein extracts from intestine, but not in those from *X. laevis* oocytes, two additional weaker bands of ~31 and 39 kDa were detected. The 31-kDa band might correspond to a glycosylated form, since SaAqp1a shows a glycosylation motif in extracellular loop E (Asn^{194}; Fig. 1*B*), whereas the 39-kDa band could be a dimer (22, 49). Control blots incubated with the SaAqp1a antisera preadsorbed with large amounts of the immunizing peptide were negative (Fig. 2*B*, *right*), indicating the specificity of the reaction.

Immunoblotting with the same protein extracts and the SaAqp1b antisera identified two very close immunoreactive bands with a molecular mass of ~27 and 29 kDa in oocytes injected with SaAqp1b, in agreement with the calculated molecular mass (27.2 kDa) of the SaAqp1b amino acid sequence deduced from its cDNA (Fig. 2*C*, *left, lane 3*). Lanes from the same blot corresponding to water- and SaAqp1a-injected

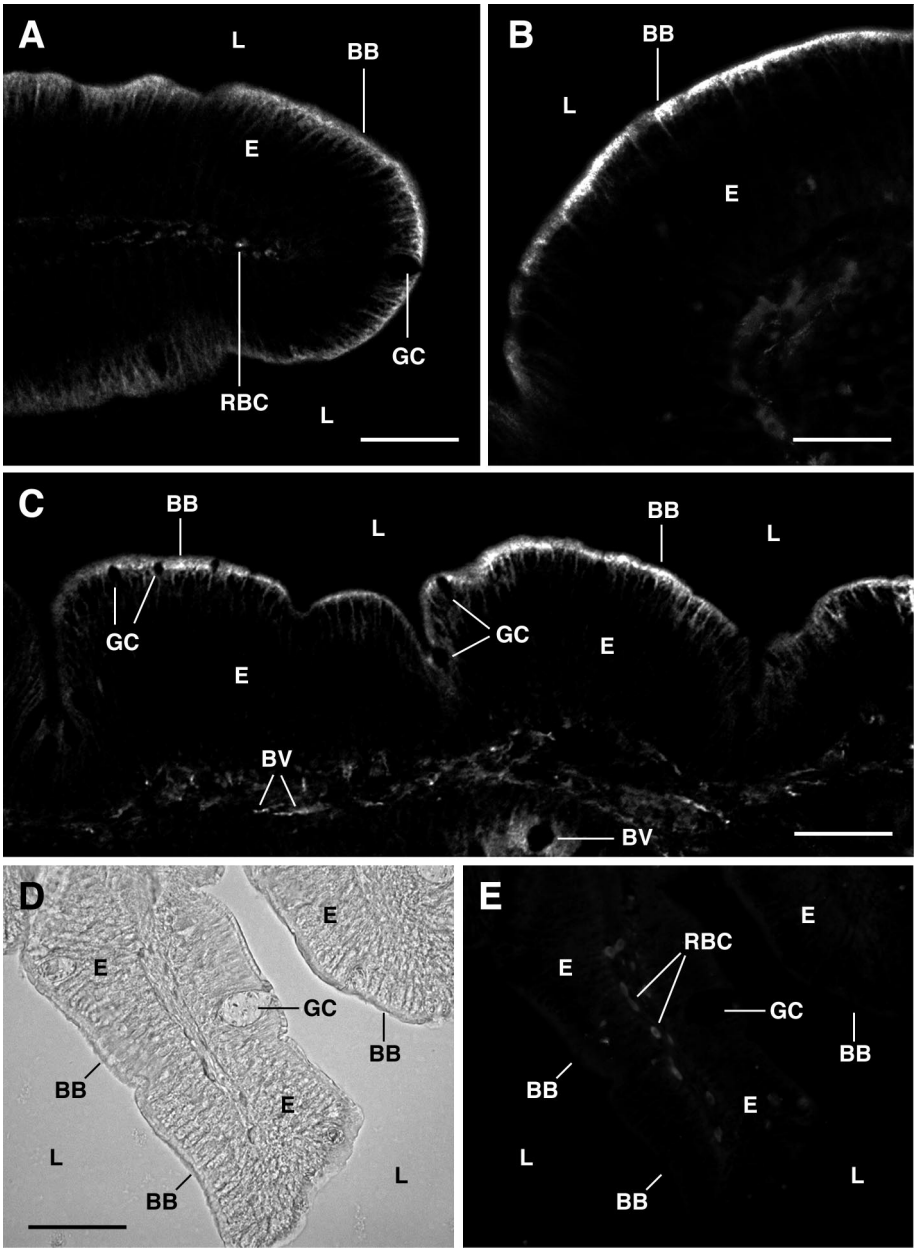

Fig. 3. Immunofluorescence microscopy on paraffin sections from the duodenum (*A* and *B*) and hindgut (*C*) of SW-acclimated seabream ($n = 3$ fish) after reaction with the SaAqp1a antisera. In *D* (phase contrast) and *E* (epifluorescence) is shown a control section from hindgut incubated with peptide-negated antiserum. The same negative results were obtained with the preimmune serum (not shown). BB, brush border; BV, blood vessel; E, epithelium; GC, goblet cell; L, lumen; RBC, red blood cells. Bars, 100 μm (*A, C and D*), 20 μm (*B*).

oocytes were negative (Fig. 2*C*, *left, lanes 1* and *2*), thus confirming the absence of cross-reaction between the SaAqp1a and SaAqp1b antisera. In total membrane extracts from seabream duodenum and hindgut, a single SaAqp1b immunoreactive band of ~28 kDa was observed, whereas in the rectum two prominent bands of 27 and 29 kDa, apparently the same that were observed in oocyte extracts, were detected (Fig. 2*C*, *left, lanes D, H*, and *R*). The intensity of the single bands in the duodenum and hindgut was lower than that of the double bands present in the rectum. Control blots incubated with preadsorbed SaAqp1b antisera did not show any protein band (Fig. 2*C*, *right*).

Cellular localization of SaAqp1a and SaAqp1b in the intestine. The cellular distribution of both SaAqp1a and SaAqp1b in the seabream intestine was characterized by immunofluorescence light microscopy. In the duodenum and hindgut, an intense SaAqp1a immunoreactivity was detected in the apical brush border of epithelial cells, suggesting that SaAqp1a was localized on or very close to the apical microvilli (Fig. 3, *A–C*). The lateral membrane of the columnar epithelial cells also showed SaAqp1a immunofluorescence, although the intensity was apparently lower than in the brush border. Specific SaAqp1a immunostaining was also detected in endothelial cells of blood vessels within the submucosa and muscular layers (Fig. 3*C*). The goblet intestinal cells, however, were negative for SaAqp1a staining (Fig. 3, *A* and *C*). The SaAqp1b immunoreactivity in the duodenum and hindgut was detected specifically in the brush border of the epithelial cells (Fig. 4, *A* and *B*). However, there was a considerable variability in the intensity of the SaAqp1b immunoreaction in these regions, the signal being in general much weaker than that observed by using the SaAqp1a antisera, even after a detergent permeabilization of the histological sections before incubation with the primary antibody. Unlike for SaAqp1a, vascular endothelia and red blood cells were apparently devoid of SaAqp1b (Fig. 4, *A* and *B*).

In the rectum, a different pattern of SaAqp1a localization with respect to that found in the duodenum and hindgut was observed. In this region, strong SaAqp1a staining was detected almost exclusively in the intracellular subapical compartment of some specific epithelial cells randomly distributed within the epithelia as well as located at the base of the intervillus pockets (Fig. 5, *A* and *C*), which are possibly analogous to crypts of Lieberkühn from mammals (8). These cells had a more rounded nucleus, with a well visible nucleolus, and a lower amount of eosinophilic (i.e., basic) granules in the subapical compartment than columnar enterocytes (Fig. 5*D*). A faint SaAqp1a staining was, however, also observed in the perinuclear compartment, as well as in the apical brush border and lateral membrane, of enterocytes containing many eosinophilic granules outside of the intestinal folds (Fig. 5*B*). By contrast, the SaAqp1b antisera intensively stained the brush border of both types of rectal enterocytes, indicating a restricted localization of SaAqp1b in the apical membrane (Fig. 6, *A–C*). As it occurred in the duodenum and hindgut, the endothelial cells of blood vessels from the rectum were also strongly stained with the SaAqp1a (Fig. 5*A*) antisera but not with the SaAqp1b antisera, and there were no apparent differences in SaAqp1a immunoreactivity in these areas between rectum, duodenum, and hindgut. The immunohistochemistry results were thus consistent with previous qPCR and Western blotting analysis indicating that the rectum showed the lowest abundance of SaAqp1a and the highest abundance of SaAqp1b. This may be caused by the accumulation of SaAqp1a mainly in the cyto-

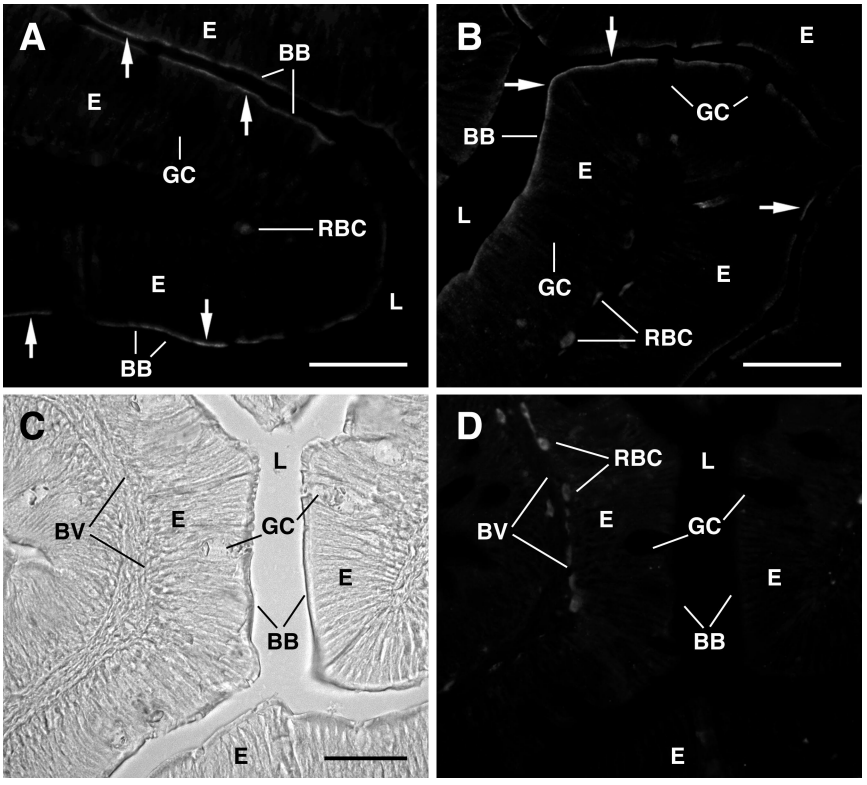

Fig. 4. Immunofluorescence microscopy on paraffin sections from the duodenum (*A*) and hindgut (*B*) of SW-acclimated seabream ($n = 3$ fish) after reaction with the SaAqp1b antisera. In *C* and (phase contrast) and *D* (epifluorescence) is shown a control section from hindgut incubated with peptide-negated antiserum. The same negative results were obtained with the preimmune serum (not shown). Note that SaAqp1b reaction in the duodenum and hindgut is very weak (arrows) even after permeabilization of the tissue sections with SDS (see MATERIALS AND METHODS). Bars, 100 μm (*A–C*).

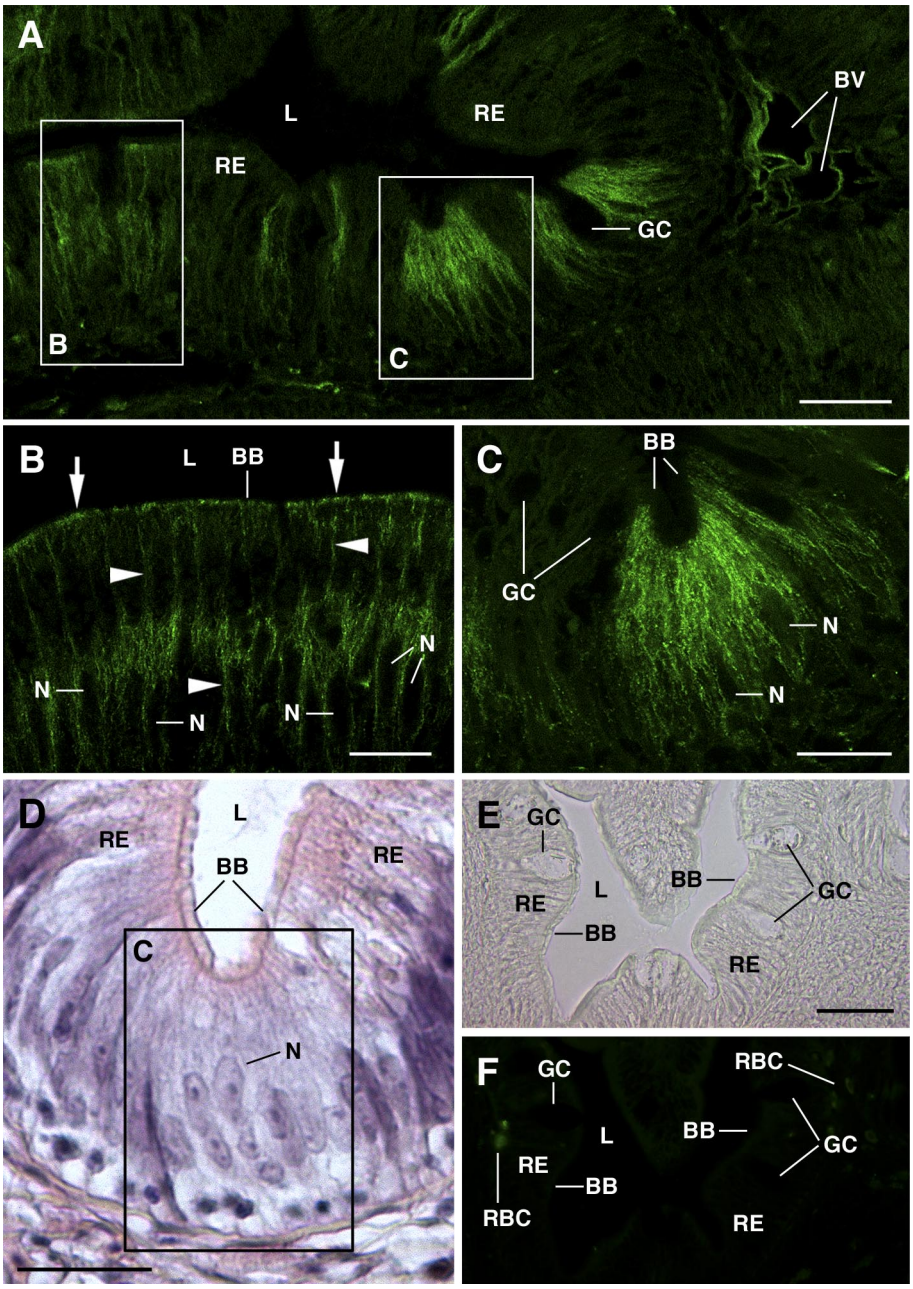

Fig. 5. Immunofluorescence microscopy on paraffin sections from the rectum of SW-acclimated seabream ($n = 3$ fish) after reaction with the SaAqp1a antisera. *B* and *C* correspond to the regions indicated in *A*. In *B*, arrows point the apical membrane of enterocytes, whereas the arrowheads indicate lateral membrane. *D* shows a section stained with hematoxylin and eosin showing the enterocytes located at the base of the intervillus pockets. *E* (phase contrast) and *F* (epifluorescence) show a control section incubated with antigen-negated SaAqp1a. The same negative results were obtained with the preimmune serum (not shown). RE, rectal epithelium; N, nucleus of enterocytes. Bars, 100 μm (*E* and *F*), 50 μm (*A* and *E*), and 20 μm (*B–D*).

plasm of a subpopulation of rectal enterocytes, whereas SaAqp1b was highly expressed at the brush border of all enterocytes of the rectum.

Effect of FW acclimation on SaAqp1a and SaAqp1b protein abundance in the intestine. Western blotting analysis was performed employing the same antisera as before and purified cell membrane fractions from the intestine of fish maintained in SW and of fish acclimated to FW for 10 days (Figs. 7*A* and 8*A*). Quantification of immunoblots determined that FW acclimation of seabream resulted in a significant decrease in SaAqp1a expression throughout the whole intestine ($P < 0.05$), with this decrease being especially marked in the rectum (by ~80%) (Fig. 7*B*). However, FW acclimation only significantly reduced ($P < 0.05$) SaAqp1b protein abundance in the rectum (by ~50%), whereas in duodenum and hindgut the levels of this protein remained unchanged (Fig. 8*B*).

DISCUSSION

It is well established that AQP water channels are a family of membrane proteins that facilitate water movement across cell membranes in plants and animals (1). Thus far, at least 13 distinct AQPs have been discovered in mammals, from which some are water selective (AQP0, -1, -2, -4, -5, -6, and -8), some are aquaglyceroporins (AQP3, -7, -9, and -10), and two (AQP11 and -12) belong to a closely related subfamily in which permeability properties have not yet been conclusively characterized (1, 21, 51). Recent efforts to clone and characterize teleost AQPs indicate the expression of two different AQP1 orthologs in this group of vertebrates (13, 37), unlike in mammals, as well as a number of different aqualyceroporin paralogs (4, 10–12, 15, 36, 37, 43, 50). However, the permeability properties of most fish AQPs and aquaglyceroporins

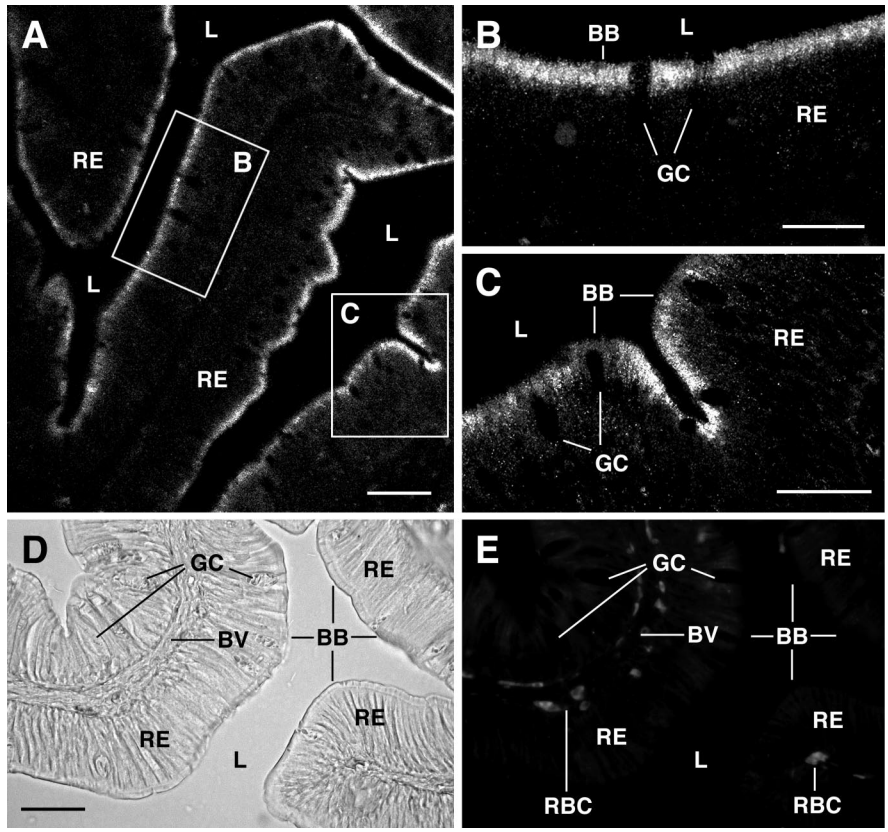

Fig. 6. Immunofluorescence microscopy on paraffin sections from the rectum of SW-acclimated seabream ($n = 3$ fish) after reaction with the SaAqp1b antisera. *B* and *C* correspond to the regions indicated in *A*. *D* (phase contrast) and *E* (epifluorescence) show a control section incubated with antigen-negated SaAqp1b. The same negative results were obtained with the preimmune serum (not shown). Bars, 50 μm (*A, D*, and *E*) and 20 μm (*B* and *C*).

have not been reported yet, which makes understanding of their physiological roles difficult. Based on phylogenetic and genomic analysis, we have recently proposed to name the two fish AQP1 orthologs as Aqp1a and Aqp1b, with the latter group including the SaAqp1o and the European eel Aqp1dup (7, 47). In the present work, it is shown that SaAqp1a and SaAqp1b are both water-selective channels with permeability properties similar to those of human AQP1, and thus they can be classified as true AQP1 paralogs.

The gilthead seabream has a short intestine that is largely divided into two regions, the anterior intestine or duodenum and the posterior intestine or hindgut (6). After the posterior intestine, there is a narrowing corresponding to a valve, marking the pass to the rectum. The epithelia of the duodenum and hindgut is typically folded, forming the villi that protrude into the lumen and the intervillus pockets, and it consists of columnar cells, the enterocytes, intercalated with the mucus-secreting goblet cells, which increase in number toward the lower part of the intestine (6). The rectal epithelia is also folded and is characterized by enterocytes containing many vacuoles filled with eosinophilic granules. This study showed that SaAqp1a was expressed in epithelial enterocytes from all intestinal segments of SW-acclimated seabream, with the duodenum and hindgut showing the highest mRNA and protein levels. The presence of Aqp1a in fish intestinal enterocytes agrees with previous reports in SW-acclimated eels and sea bass, where the Aqp1a ortholog is mainly expressed by columnar enterocytes of the posterior intestine, whereas Aqp3 is found in intraepithelial "macrophage-like" and goblet cells of the rectal epithelium (4, 15, 29, 36). These findings, however, contrast with the situation in mammals, where AQP1 has not been reported in normal epithelial cells lining the gastrointestinal system but exclusively in microvascular endothelia (30, 39). The localization of AQP1 in gastrointestinal epithelial cells has only been demonstrated in tumors of the colon, where it seems to contribute to tumor angiogenesis and the formation of high fluid pressures and high vascular permeability of tumor microvessels (40). The differences in the intestinal localization of AQP1 between fish and mammals are probably related to the fact that the gastrointestinal tract of teleosts plays an important osmoregulatory role (17).

Water absorption across the marine teleost intestine is tightly linked to the absorption of Na^+ in the enterocytes fueled by the basolateral Na^+-K^+-ATPase, which provides the energy necessary for the active transport of K^+ and Cl^- from the intestinal lumen by apical cotransporters (17). The highest abundance of SaAqp1a protein in the duodenum and hindgut, mostly located at the apical plasma membrane of enterocytes, suggests that in seabream these intestinal regions may play a major role in SaAqp1a-mediated water absorption following the uptake of ions. This conclusion would be consistent with earlier reports which indicate that the highest levels of water flux within the teleost intestine occur in the midregion, followed in descending order by the posterior and anterior intestine, and finally the rectum (2, 3). The seabream aquaglyceroporin sbAQP, however, is not likely to be involved in water transport across the intestinal epithelia, since its mRNA is found only in cells scattered in the lamina propria and at the interface of the circular and longitudinal muscle layer of the hindgut (43). In SW-acclimated silver eels, as in seabream, the rectal epithelium shows low Aqp1a expression, whereas the posterior/rectal intestinal segment exhibits the highest amount

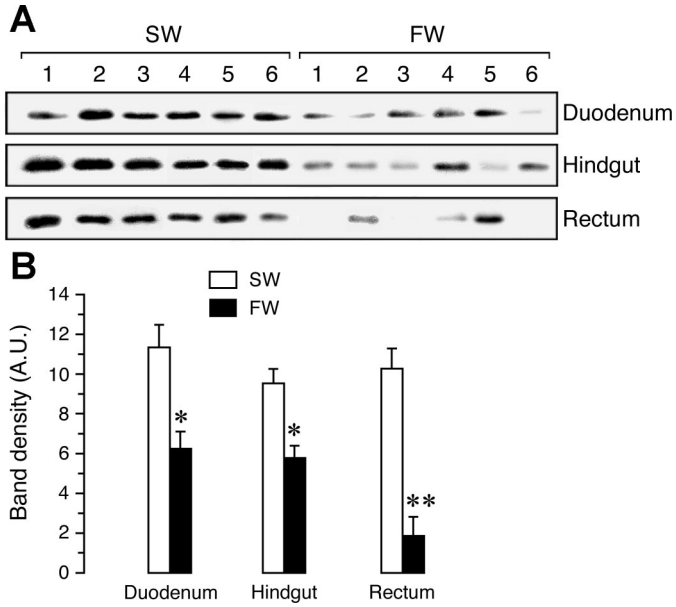

Fig. 7. Effect of freshwater (FW) acclimation on SaAqp1a abundance in the duodenum, hindgut, and rectum. *A*: representative Western blot of protein extracts (20 μg) of total membranes from different parts of the intestine from 6 fish maintained in SW or acclimated in FW for 10 days. Three separate membranes, for duodenum, hindgut, and rectum, each containing protein extracts from SW- and FW- acclimated fish, were exposed to X-ray films for different times to optimize the signal intensity. *B*: quantitative analysis of intestinal SaAqp1a protein expression from data shown in A. Values are means ± SE ($n = 6$). Data of FW-acclimated fish with asterisks are significantly different from those of SW-acclimated fish (Student's *t*-test; $*P < 0.05$ and $**P < 0.01$).

of Aqp1a mRNA and protein (36). In this intestinal segment of the eel, Aqp1a localizes preferentially in the apical membrane of epithelial cells, which is consistent with the highest water absorption rates found in the eel posterior intestine (4, 36). In this species, expression of AQPe, a putative aquaglyceroporin, is found in all intestinal segments, but its cellular localization is unknown (36).

Unlike in duodenum and hindgut, SaAqp1a immunoreactive peptides in rectum mainly accumulated in the cytoplasm, surrounding the nucleus, of groups of enterocytes spread within the epithelia and located at the base of the intervillus pockets. In the rest of enterocytes, much weaker SaAqp1a immunoreaction was found within the perinuclear compartment and in the apical brush border and lateral plasma membrane. In fish, intestinal stem cells, responsible for the renewal of the gut epithelium, are confined to the base of the intervillus pockets, which also contains stem cell dividing offspring-committed progenitors undergoing divisions before terminal differentiation (8). Thus the cells located at the base of the rectal pockets showing SaAqp1a cytoplasmic localization could correspond to intestinal progenitors committed to differentiate into enterocytes. The localization of Aqp1a in these cells has not been reported in any other fish species; therefore, the precise nature of these cells awaits further investigation.

In the European eel, mRNA encoding Aqp1dup (i.e., the eel Aqp1b paralog) is accumulated in the esophagus and kidney, but it has not been found in the intestine of either FW- or SW-adapted eels by using semiquantitative Northern blot (37, 38). In SW-acclimated seabream, we have found that *aqp1b* mRNA is expressed in the different segments of the intestine, although the rectum showed the highest levels. Such a discrepancy with the data reported in eel is possibly caused by the lower expression level of *aqp1b* mRNA in the intestine of SW-adapted eels when compared with that in esophagus or kidney (47), which may only be detected by qPCR. In the seabream, according with the mRNA levels, the highest abundance of SaAqp1b protein was observed in rectum, where two bands possibly corresponding to phosphorylated and nonphosphorylated forms (47) were detected, although some variability between fish was also observed. However, Western blotting analysis of membrane fractions from duodenum and hindgut revealed the presence of one single SaAqp1b reactive band migrating approximately between the two bands present in membrane fractions from SaAqp1b-injected *X. laevis* oocytes, expressing functional SaAqp1b, and rectum. Interestingly, SaAqp1b was poorly detected by immunofluorescence microscopy in duodenum and hindgut. Recent studies using heterologous expression in *X. laevis* oocytes have shown that expression of SaAqp1b bearing a mutated COOH terminus that induces its retention in the endoplasmic reticulum (ER) and partial degradation results in an identical electrophoretic profile (47). Thus the unusual electrophoretic profile of SaAqp1b extracted from the duodenum and hindgut, together with its poor immunocytochemical detection, suggests that the protein detected by Western blot in these intestinal segments may be retained in the ER and thus not functional.

In the rectum, SaAqp1b immunostaining was restricted exclusively to the apical brush border of the enterocytes, and thus it showed a distinct distribution than SaAqp1a in this intestinal region. Interestingly, FW adaptation produced a reduction in

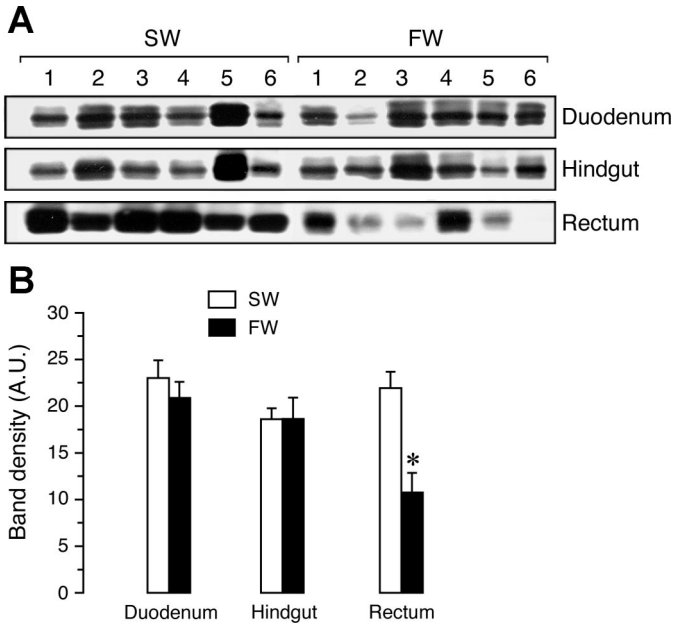

Fig. 8. Effect of FW acclimation on SaAqp1b abundance in the duodenum, hindgut, and rectum. *A*: representative Western blot of protein extracts (20 μg) of total membranes from different parts of the intestine from 6 fish maintained in SW or acclimated in FW for 10 days. Western blots were carried out as described in Fig. 7. *B*: quantitative analysis of intestinal SaAqp1b protein expression from data shown in *A*. Values are means ± SE ($n = 6$). Data of FW-acclimated fish with an asterisk are significantly different from those of SW-acclimated fish (Student's *t*-test; $*P < 0.05$).

SaAqp1b protein abundance in the rectum (by ~50%) but not in the duodenum or hindgut. The eel *aqp1b* mRNA expression in esophagus is upregulated after cortisol treatment, whereas in the kidney both *aqp1a* and *aqp1b* transcripts are downregulated after cortisol infusion or SW acclimation (37). These findings thus suggest that, although teleost Aqp1b seems to be a specialized AQP involved in water uptake by the oocyte during steroid-induced meiotic maturation (13, 14), it may also play other osmoregulatory roles in somatic tissues, such as water absorption across the rectal epithelium. Based on the relative amount of SaAqp1a and SaAqp1b peptides along the entire length of the seabream intestine, it is possible to speculate that, in the rectum, SaAqp1a may have a limited role in water absorption leaving to SaAqp1b the bulk of water transport. However, the synthesis of SaAqp1b, although maybe not functional, also occurred in the duodenum and hindgut and was apparently not altered by changes in salinity. Future studies will be necessary to elucidate the mechanisms involved in SaAqp1b protein synthesis and sorting into the plasma membrane in intestinal enterocytes, as well as the physiological significance of SaAqp1a and SaAqp1b coexpression in rectal enterocytes, which remains intriguing.

The immunocytochemical detection of SaAqp1a and SaAqp1b in the epithelial intestine of seabream, as well as of Aqp1a in other teleosts (4, 36), may favor the hypothesis of a transcellular pathway during the active water transport mechanism in the intestine under high-salinity conditions. Although the presence of an AQP-mediated mechanism in the fish intestine has not been yet functionally demonstrated, it may be supported by the observation that SW conditions induce *aqp1a* and *aqp1b* mRNA expression and/or protein synthesis in the intestinal epithelium (4, 15, 36, and the present work). Moreover, it has been shown that injection of cortisol in FW eels upregulates the expression of Aqp1a throughout the intestine and elevates intestinal permeability with commensurate increases in the net absorption of monovalent ions and water (19, 36, 48). The presence of Aqp1a in vascular endothelia within the submucosa and muscular layers of the intestine (4, 36, and the present work) may provide an additional exit pathway for water absorbed by the intestinal epithelia to flow in the blood circulation. However, the present and previous works have failed to conclusively demonstrate the presence of AQPs in the basal membrane of teleost enterocytes which might be required to transport water across the intestinal epithelia. Therefore, the investigation of the presence of additional AQPs in the fish intestine is necessary to gain a more complete understanding of the anatomical localization and molecular identity of AQPs in the teleost gastrointestinal tract as well as of their functions.

Perspectives and Significance

This study is the first to demonstrate the differential expression, localization, and regulation during FW acclimation of two teleost-specific AQP1 homologs, Aqp1a and Aqp1b, in the enterocytes along the intestine of an euryhaline teleost. Although direct experimental evidence is still lacking, these findings provide further support for the role of AQP1-like channels in mediating water absorption across the intestine of SW-acclimated fish. However, based on the relative abundance of mRNA and protein along the intestine, in addition to their specific cellular localization, it is intriguing to speculate that SaAqp1a and SaAqp1b may play specialized roles in duodenum/hindgut and rectum, respectively, for water absorption. The present and previous studies thus suggest that teleost Aqp1b has possibly been neofunctionalized in some osmoregulatory cells (i.e., oocytes and rectal enterocytes) following gene duplication. Future studies will be necessary to elucidate the physiological significance of this evolutionary process within the teleost lineage, as well as the associated isoform-specific regulatory mechanisms, which will help understand the osmoregulatory adaptations underlying the vertebrate radiation.

ACKNOWLEDGMENTS

Present addresses: D. Raldúa, Laboratory of Environmental Toxicology, Universidad Politécnica de Catalunya, Ctra. Nac. 150, km. 14.5 -Zona IPCT, TR-23 -Campus Terrassa, 08220 Terrassa, Spain; and M. Fabra, Department of Genetic Medicine and Development, 8242 CMU, 1 rue Michel Servet, University of Geneva Medical School, 1211 Geneva 4, Switzerland.

GRANTS

This work was supported by Grants from the Spanish Ministry of Education and Science (MEC; AGL2001-0364/ACU and AGL2004-00316) and the European Commission (Q5RS-2002-00784-CRYOCYTE) and by the Reference Center in Aquaculture (Generalitat de Catalunya, Spain) to J. Cerdà. Participation of M. Fabra and D. Raldúa was financed by a fellowship from the Catalan Government (DURSI, Spain) and by a "Ramón y Cajal" contract (MEC), respectively.

REFERENCES

1. **Agre P, King SL, Yasui M, Guggino WB, Ottersen OP, Fujiyoshi Y, Engel A, Nielsen S.** Aquaporin water channels - from atomic structure to clinical medicine. *J Physiol* 542: 3–16, 2002.
2. **Ando M.** Chloride-dependent sodium and water transport in the seawater eel intestine. *J Comp Physiol* 138B: 87–91, 1980.
3. **Ando M, Kobayashi M.** Effects of stripping of the outer layers of the eel intestine on salt and water transport. *Comp* Physiol Biochem 61A: 497–501, 1978.
4. **Aoki M, Kaneko T, Katoh F, Hasegawa S, Tsutsui N, Aida K.** Intestinal water absorption through aquaporin 1 expressed in the apical membrane of mucosal epithelial cells in seawater-adapted Japanese eel. *J Exp Biol* 206: 3495–3505, 2003.
5. **Bentley PJ.** *Endocrines and Osmoregulation*. *Zoophysiology*. Berlin: Springer, vol. 39, 2002.
6. **Cataldi E, Cataudella S, Monaco G, Rossi A, Tancioni L.** A study of the histology and morphology of the digestive tract of the sea-bream, *Sparus aurata*. *J Fish Biol* 30: 135–145, 1987.
7. **Cerdà J, Fabra M, Raldúa D.** Physiological and molecular basis of fish oocyte hydration. In: *The Fish Oocyte: From Basic Studies to Biotechnological Applications*, edited by Babin P, Cerdà J, and Lubzens E. The Netherlands: Springer, 2007, p. 349–396.
8. **Crosnier C, Vargesson N, Gschmissner S, Ariza-McNaughton L, Morrison A, Lewis J.** Delta-Notch signalling controls commitment to a secretory fate in zebrafish intestine. *Development* 132: 1093–1104, 2005.
9. **Cutler C, Cramb G.** Water transport and aquaporin expression in fish. In: *Molecular Biology and Physiology of Water and Solute Transport*, edited by Hohmann S, Nielsen S, and Agre P. London: Kluwer, 2000, p. 431–441.
10. **Cutler CP, Cramb G.** Branchial expression of an aquaporin 3 (AQP-3) homologue is downregulated in the European eel *Anguilla anguilla* following seawater acclimation. *J Exp Biol* 205: 2643–2651, 2002.
11. **Cutler CP, Martinez AS, Cramb G.** The role of aquaporin 3 in teleost fish. *Comp Biochem Physiol* 148A: 82–91, 2007.
12. **Deane EE, Woo NYS.** Tissue distribution, effects of salinity acclimation, and ontology of aquaporin 3 in the marine teleost, silver sea bream (*Sparus sarba*). *Mar Biotech* 8: 1–9, 2006.
13. **Fabra M, Raldúa D, Power DM, Deen PM, Cerdà J.** Marine fish egg hidration is aquaporin-mediated (Abstract). *Science* 307: 545, 2005.
14. **Fabra M, Raldúa D, Bozzo MG, Deen PM, Lubzens E, Cerdà J.** Yolk proteolysis and aquaporin-1o play essential roles to regulate fish oocyte hydration during meiosis resumption. *Dev Biol* 295: 250–262, 2006.

15. **Giffard-Mena I, Boulo V, Aujoulat F, Fowden H, Castille R, Charmantier G, Cramb G.** Aquaporin molecular characterization in the sea-bass (*Dicentrachus labrax*): the effect of salinity on AQP1 and AQP3 expression. *Comp Biochem Physiol* 148A: 430–444, 2007.
16. **Gonen T, Walz T.** The structure of aquaporins. *Q Rev Biophys* 39: 361–396, 2006.
17. **Grosell M.** Intestinal anion exchange in marine fish osmoregulation. *J Exp Biol* 209: 2813–2827, 2006.
18. **Hirano T, Mayer-Gostan N.** Eel esophagus as an osmoregulatory organ. *Proc Natl Acad Sci USA* 73: 1348–1350, 1976.
19. **Hirano T, Morisawa M, Ando M, Utida S.** Adaptive changes in ion and water transport mechanism in the eel intestine. In: *Intestinal Ion Transport*, edited by Robinson JWL. London: Kluwer, 1976, p. 301–317.
20. **Hirata T, Kaneko T, Ono T, Nakazato T, Furukawa N, Hasegawa S, Wakabayashi S, Shigekawa M, Chang MH, Romero MF, Hirose S.** Mechanism of acid adaptation of a fish living in a pH 3.5 lake. *Am J Physiol Regul Integr Comp Physiol* 284: R1199–R1212, 2003.
21. **Ishibashi K.** Aquaporin subfamily with unusual NPA boxes. *Biochim Biophys Acta* 1758: 989–993, 2006.
22. **Jin SY, Liu YL, Xu LN, Jiang Y, Wang Y, Yang BX, Yang H, Ma TH.** Cloning and characterization of porcine aquaporin 1 water channel expressed extensively in gastrointestinal system. *World J Gastroenterol* 12: 1092–1097, 2006.
23. **Kamsteeg EJ, Deen PM.** Detection of aquaporin-2 in the plasma membranes of oocytes: a novel isolation method with improved yield and purity. *Biochem Biophys Res Commun* 282: 683–690, 2001.
24. **Klaren PH, Guzman JM, Reutelingsperger SJ, Mancera JM, Flik G.** Low salinity acclimation and thyroid hormone metabolizing enzymes in gilthead seabream (*Sparus auratus*). *Gen Comp Endocrinol* 152: 215–22, 2007.
25. **Kleszczynska A, Vargas-Chacoff L, Gozdowska M, Kalamarz H, Martinez-Rodríguez G, Mancera JM, Kulczykowska E.** Arginine vasotocin, isotocin and melatonin responses following acclimation of gilthead sea bream (*Sparus aurata*) to different environmental salinities. *Comp Biochem Physiol Mol Integr Physiol* 145A: 268–73, 2006.
26. **Laemmli UK.** Cleavage of structural proteins during the assembly of the head of bacteriophage T4. *Nature* 227: 680–685, 1970.
27. **Laiz-Carrión R, Martín del Río MP, Miguez, JM, Mancera, JM, Soengas JL.** Influence of cortisol on osmoregulatoin and energy metabolism in gilhead sea beam *Sparus auratus*. *J Exp Zool* 298: 105–118, 2003.
28. **Laiz-Carrión R, Guerreiro PM, Fuentes J, Canario AV, Martin Del Rio MP, Mancera JM.** Branchial osmoregulatory response to salinity in the gilthead sea bream, *Sparus auratus*. *J Exp Zool* 303A: 563–76, 2005.
29. **Lignot JH, Cutler CP, Hazon N, Cramb G.** Immunolocalisation of aquaporin 3 in the gill and the gastrointestinal tract of the European eel *Anguilla anguilla* (L.). *J Exp Biol* 205: 2653–2663, 2002.
30. **Ma T, Verkman AS.** Aquaporin water channels in gastrointestinal physiology. *J Physiol* 517: 317–326, 1999.
31. **Mancera JM, Pérez-Fígares JM, Fernández-Llebrez P.** Osmoregulatory responses to abrupt salinity changes in the euryhaline gilthead sea bream (*Sparus auratus*). *Comp Biochem Physiol* 106A: 245–250, 1993.
32. **Mancera JM, Fernández-Llebrez P, Grondona JM, Pérez-Fígares JM.** Influence of environmental salinity on prolactin and corticotropic cells in the euryhaline gilthead sea bream (*Sparus auratus L*). *Gen Comp Endocrinol* 90: 220–231, 1993.
33. **Mancera JM, Pérez-Fígares JM, Fernández-Llebrez P.** Effect of cortisol on brackish water adaptation in the euryhaline gilthead sea bream (*Sparus auratus* L.). *Comp Biochem Physiol* 107A: 397–402, 1994.
34. **Mancera JM, Pérez-Fígares JM, Fernández-Llebrez P.** Effect of decreased environmental salinity on growth hormone cells in the euryhaline gilthead sea bream (*Sparus auratus L*). *J Fish Biol* 46: 494–500, 1995.
35. **Mancera JM, Laiz-Carrión R, Martín del Río MP.** Osmoregulatory action of PRL, GH, and cortisol in the gilthead seabream (*Sparus auratus L*). *Gen Comp Endocrinol* 129: 95–103, 2002.
36. **Martinez AS, Cutler CP, Wilson GD, Phillips C, Hazon N, Cramb G.** Regulation of expression of two aquaporin homologs in the intestine of the European eel: effects of seawater acclimation and cortisol treatment. *Am J Physiol Regul Integr Comp Physiol* 288: R1733–R1743, 2005.
37. **Martinez AS, Cutler CP, Wilson GD, Phillips C, Hazon N, Cramb G.** Cloning and expression of three aquaporin homologues from the European eel (*Anguilla anguilla*): effects of seawater acclimation and cortisol treatment on renal expression. *Biol Cell* 97: 615–627, 2005.
38. **Martinez AS, Wilson G, Phillips C, Cutler C, Hazon N, Cramb G.** Effect of cortisol on aquaporin expression in the esophagus of the European eel, *Anguilla anguilla*. *Ann NY Acad Sci* 1040: 395–398, 2005.
39. **Mobasheri A, Marples D.** Expression of the AQP-1 water channel in normal human tissues: a semiquantitative study using tissue microarray technology. *Am J Physiol Cell Physiol* 286: C529–C537, 2004.
40. **Mobasheri A, Airley R, Hewitt SM, Marples D.** Heterogeneous expression of the aquaporin 1 (AQP1) water channel in tumors of the prostate, breast, ovary, colon and lung: a study using high density multiple human tumor tissue microarrays. *Int J Oncol* 26: 1149–1158, 2005.
41. **Preston GM, Carroll TP, Guggino WB, Agre P.** Appearance of water channels in *Xenopus* oocytes expressing cell CHIP28 protein. *Science* 256: 385–387, 1992.
42. **Preston GM, Jung JS, Guggino WB, Agre P.** The mercury-sensitive residue at cysteine 189 in the CHIP28 water channel. *J Biol Chem* 268: 17–20, 1993.
43. **Santos CR, Estêvão MD, Fuentes J, Cardoso JC, Fabra M, Passos AL, Detmers FJ, Deen PM, Cerdà J, Power DM.** Isolation of a novel aquaglyceroporin from a marine teleost (*Sparus auratus*): function and tissue distribution. *J Exp Biol* 207: 1217–1227, 2004.
44. **Skadhauge E.** The mechanism of salt and water absorption in the instestine of the eel (*Anguilla anguilla*) adapted to waters of various salinities. *J Physiol* 204: 135–158, 1969.
45. **Skadhauge E.** Coupling of transmural flows of NaCl and water in the intestine of the eel (*Anguilla anguilla*). *J Exp Biol* 60: 535–546, 1974.
46. **Sui H, Han BG, Lee JK, Walian P, Jap BK.** Structural basis of water-specific transport through the AQP1 water channel. *Nature* 414: 872–878, 2001.
47. **Tingaud-Sequeira A, Fabra M, Otero D, Cerdà J.** Identification and characterization of a novel subfamily of aquaporin-1-related water channels neofunctionalized in oocytes of marine and catadromous teleosts. In: *Proc. 8th Int. Symp Reproductive Physiology of Fish*, edited by Roudaut G, Labbé C, and Bobe J. St. Malo, France, 2007, p. 64.
48. **Utida S, Hirano T, Oide H, Ando M, Johnson DW, Bern HA.** Hormonal control of the intestine and urinary bladder in teleost osmoregulation. *Gen Comp Endocrinol* 16: 566–573, 1972.
49. **van Hoek AN, Wiener MC, Verbavatz JM, Brown D, Lipniunas PH, Townsend RR, Verkman AS.** Purification and structure-function analysis of native, PNGase F-treated, and endo-beta-galactosidase-treated CHIP28 water channels. *Biochemistry* 34: 2212–2219, 1995.
50. **Watanabe S, Kaneko T, Aida K.** Aquaporin-3 expressed in the basolateral membrane of gill chloride cells in Mozambique tilapia *Oreochromis mossambicus* adapted to freshwater and seawater. *J Exp Biol* 208: 2673–2682, 2005.
51. **Yakata K, Hiroaki Y, Ishibashi K, Sohara E, Sasaki S, Mitsuoka K, Fujiyoshi Y.** Aquaporin-11 containing a divergent NPA motif has normal water channel activity. *Biochim Biophys Acta* 1768: 688–693, 2007.